Electronic Supplementary Information

In-situ construction of multifunctional femtosecond laser-induced graphene on arbitrary substrates

Lingxiao Wang,[a] *Kai Yin,*[*,a,b,c] *Xun Li,*[d] *Xiaolong Liu,*[e] *Jianqiang Xiao,*[a] *Jiaqing Pei,*[a] *Xinghao Song*[a]

[a] Hunan Key Laboratory of Nanophotonics and Devices, School of Physics, Central South University, Changsha 410083, China.

[b] State Key Laboratory of Precision Manufacturing for Extreme Service Performance, College of Mechanical and Electrical Engineering, Central South University, Changsha 410083, China.

[c] State Key Laboratory of Intelligent Manufacturing Equipment and Technology, Huazhong University of Science and Technology, Wuhan 430074, China.

[d] State Key Laboratory of Ultrafast Optical Science and Technology, Xi'an Institute of Optics and Precision Mechanics of CAS, Xi'an 710119, China.

[e] Department of Electronics and Nanoengineering, Aalto University, Espoo 02150, Finland.

*Corresponding author. Email: kaiyin@csu.edu.cn (Kai Yin)

Supplementary Notes

Note S1: COMSOL simulation of temperature distribution in femtosecond laser irradiating PI tape. The thermal simulations were performed using the Heat Transfer Module based on finite element method (FEM) in COMSOL Multiphysics software. In this model, the temperature after laser pulse irradiation evolution on the surface of PI tape can be described by the thermal conduction equation:

$$\rho C_p \frac{\partial T}{\partial t} + \rho C_p u \nabla T + \nabla \cdot (q) = Q \tag{S1}$$

where ρ is the density, C_p is the heat capacity, T is the temperature, **u** is the fluid flow speed, q is the heat flux density, and Q is the local heat source from the laser absorption of PI tape, respectively. Due to the femtosecond scale and extremely high temperature, the effects of heat radiation and heat conduction were mainly considered, while heat convection was neglected. The boundary condition of laser and PI interface is given by the equations:

$$-n \cdot (-k\nabla T) = Q_L \tag{S2}$$

$$-n \cdot (-k\nabla T) = \varepsilon\sigma\left(T_{amb}^4 - T^4\right) \tag{S3}$$

where k is the thermal conductivity, ε is the surface emissivity, σ is the Stefan-Boltzmann constant, T_{amb} is the ambient temperature, and Q_L is the heat flux generated by the laser respectively. The laser was modeled as an area heat source. The following equation gives the laser heat source expression:

$$Q_L = \frac{2AP_L exp\left(-\left(\frac{x^2+y^2}{r_s^2}\right)\right)}{\pi f_L r_s^2 t_L} \tag{S4}$$

where A is the laser absorption of LIG, P_L is the laser power, r_s is the laser beam radius, f_L is the laser repetition rate, and t_L is the laser pulse width, respectively. Additionally, the boundary condition of other interfaces is given by the following equation:

$$-n \cdot (-k\nabla T) = 0 \tag{S5}$$

All the relevant parameters used in the simulation were obtained from experimental data. The time step size used in the FEM calculation is 1 fs. The laser heating time was set as 350 fs.

Supplementary Figures

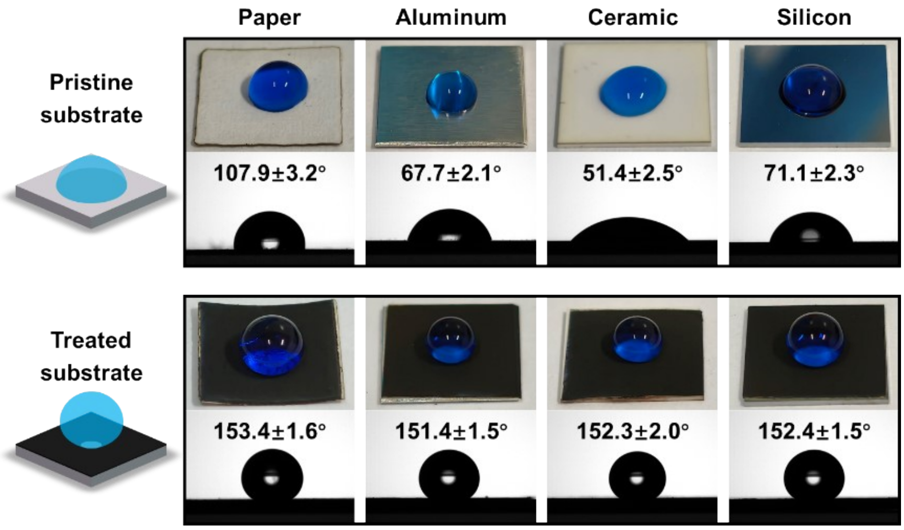

Figure S1. Water droplets placed on the pristine and treated substrates of four substrates (paper, aluminum, ceramic, and silicon); for convenience of observation, the water droplets have been stained with methylene blue.

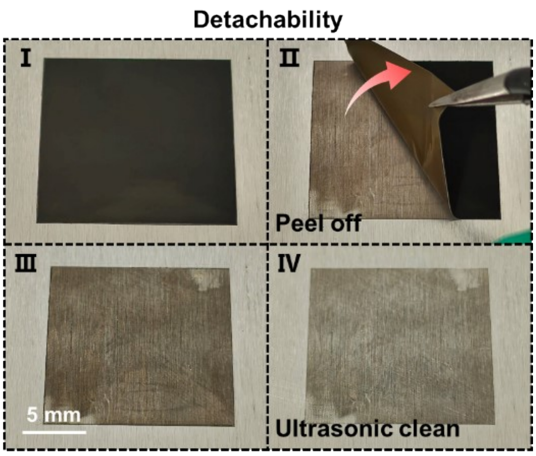

Figure S2. Detachability test of FsLIG on aluminum.

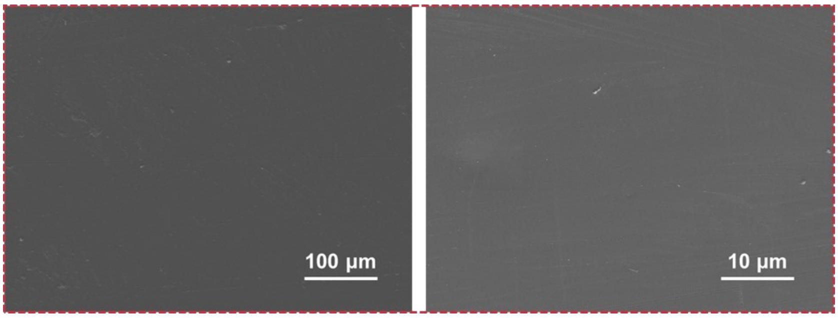

Figure S3. SEM images of the pristine PI tape surface.

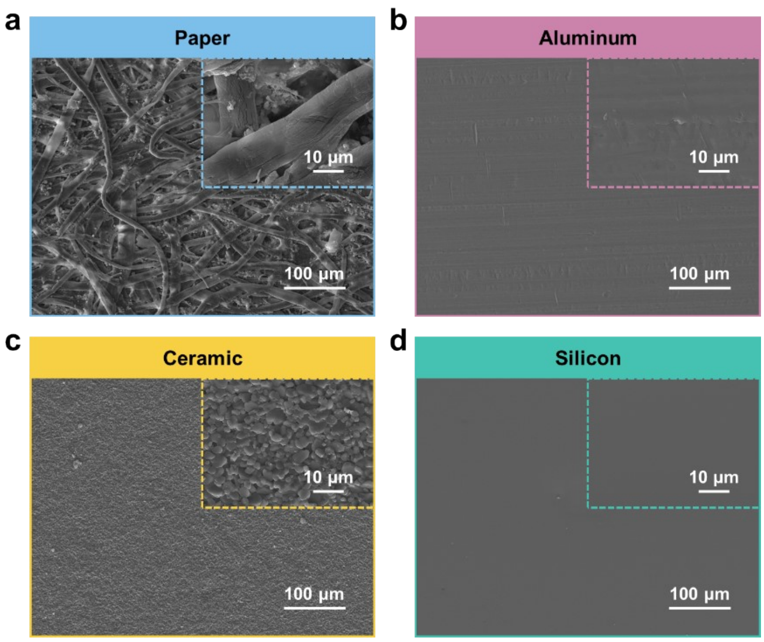

Figure S4. SEM images of pristine a) paper, b) aluminum, c) ceramic, and d) silicon surfaces.

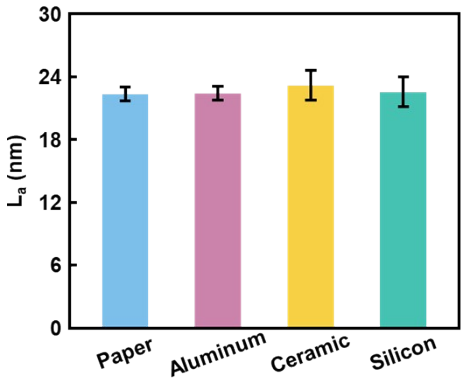

Figure S5. Calculated crystalline sizes (L_a) of FsLIG on paper, aluminum, ceramic, and silicon.

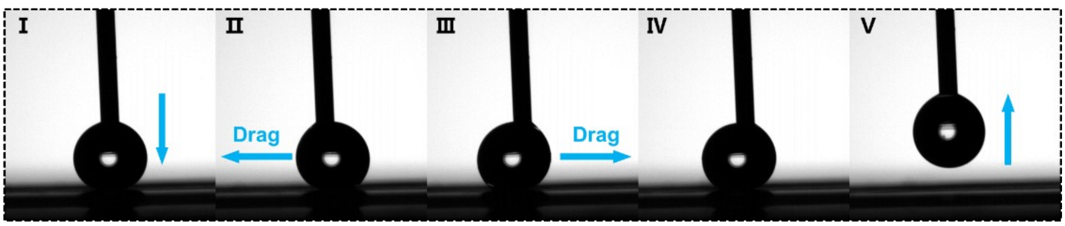

Figure S6. Dragging process and vertical anti-adhesion measurement.

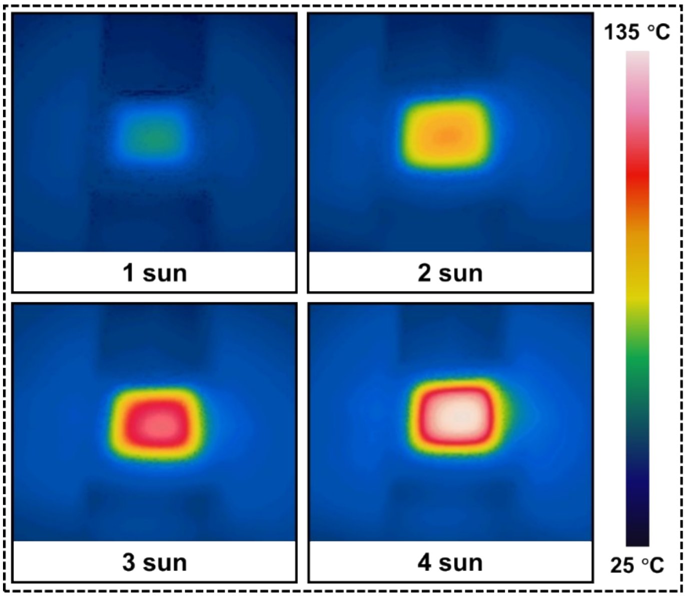

Figure S7. Infrared camera images of P-FsLIG surface under 1.0, 2.0, 3.0, and 4.0 sun illumination. The images were recorded after illumination for 240 s.

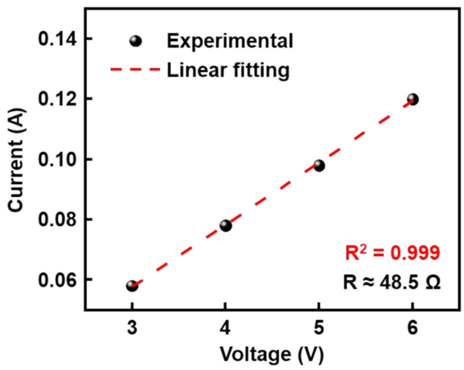

Figure S8. I−V linear curve of P-FsLIG indicating a correlation coefficient (R^2) of 0.999.

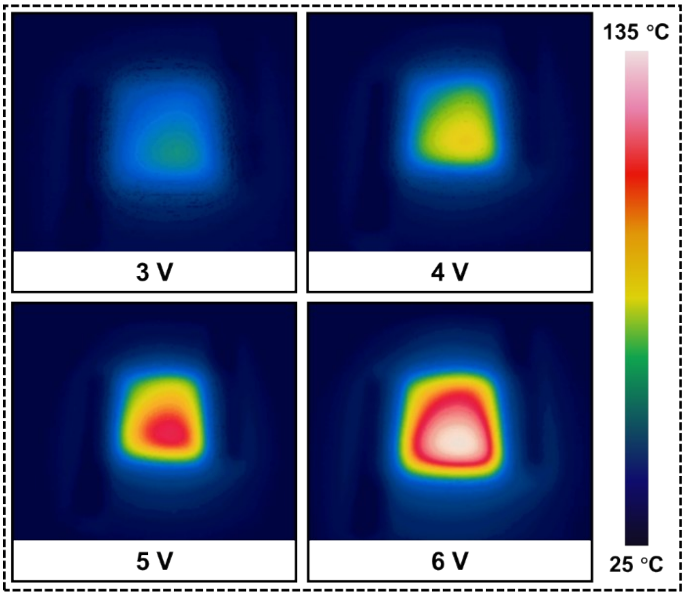

Figure S9. Infrared camera images of P-FsLIG surface at the voltages of 3, 4, 5, and 6 V. The images were recorded after applied voltage for 240 s.

Supplementary Tables

Table S1. Comparison of the FsLIG multifunctionality with other LIG materials from the literature.

Materials	Wettability	Optical Property	Electrical Property	Temperature sensing	Reference
FsLIG from PI tape	**Superhydrophobic (~153.4°)**	**~98.8% (400–1600 nm)**	**132.1 °C at 6 V 297.2 °C cm^2 W^{-1}**	**−0.089% °C^{-1} (30–80 °C)**	**This work**
TPE based LIG film	Not discussed	Not discussed	70 °C at 6 V Not given	Not discussed	S1
LIG on mask	Hydrophobic (~141°)	＞95% (300–2500 nm)	Not discussed	Not discussed	S2
LIG on glass	Not discussed	~30.0% (300–2500 nm)	~82 °C at 40 V Not given	~−0.1% °C^{-1} (30–80 °C)	S3
LIG from Kevlar	Not discussed	96.8% (190–2500 nm)	Not discussed	~−0.068% °C^{-1} (30–60 °C)	S4
LIG from wood	Not discussed	Not discussed	127.4 °C at 5 V Not given	~−0.025% °C^{-1} (30–70 °C)	S5
LIG from poly(Ph-ddm)	Superhydrophobic (~161°)	＞98.0% (250–2500 nm)	~176 °C at 4 V ~222 °C cm^2 W^{-1}	Not discussed	S6
FsLIG from PI film	Hydrophilic (~61.3°)	~98.5% (220–1400 nm)	195.7 °C at 4 V 215.9 °C cm^2 W^{-1}	Not discussed	S7
LIG from PEI film	Hydrophobic (~97°)	Not discussed	~229 °C at 7 V Not given	Not discussed	S8
AgNPs/LIG (Lased in N_2)	Hydrophobic (~140°)	~95.0% (500–2500 nm)	~46 °C at 7.5 V Not given	Not discussed	S9
Fluorine-doped LIG	Superhydrophobic (~159.2°)	Not discussed	~95 °C at 8 V ~214 °C cm^2 W^{-1}	Not discussed	S10

Note: Optical property refers to the absorption of the samples. Electrical property means the stable temperature at a specific voltage and the whole electrothermal conversion efficiency. PI: polyimide. TPE: thermoplastic elastomer. F-LIG: Forest-like LIG. PEI: polyetherimide.

Supplementary Movies

Movie S1. Self-cleaning demonstration of the P-FsLIG surface. The chalk powder was picked up by the rolling water droplets and readily removed.

Movie S2. A water droplet impacting on the P-FsLIG surface. The water droplet experienced falling, spreading, retracting, and finally rebounding back into the air.

References

[S1] Y. Li, Z. Zeng, S. Zhang, D. Guo, P. Li, X. Chen, L. Yi, H. Zheng, S. Liu, F. Liu, Highly Efficient Laser Bidirectional Graphene Printing: Integration of Synthesis, Transfer and Patterning, Small 20 (2024) 2404001.

[S2] H. Zhong, Z. Zhu, J. Lin, C. F. Cheung, V. L. Lu, F. Yan, C. Y. Chan, G. Li, Reusable and Recyclable Graphene Masks with Outstanding Superhydrophobic and Photothermal Performances, ACS Nano 14 (2020) 6213–6221.

[S3] T. Jing, H. K. Nam, D. Yang, Y. Lee, R. Gao, H. Yoo, S. Kwon, S. W. Kim, L. Yu, Y. J. Kim, In Situ Transfer of Laser-Induced Graphene Electronics for Multifunctional Smart Windows, Small Sci. 4 (2024) 2400010.

[S4] D. Yang, H. K. Nam, Y. Lee, S. Kwon, J. Lee, H. Yoon, Y. J. Kim, Laser-Induced Graphene Smart Textiles for Future Space Suits and Telescopes, Adv. Funct. Mater. 35 (2025) 2411257.

[S5] H. K. Nam, T. S. D. Le, D. Yang, B. Kim, Y. Lee, J. S. Hwang, Y. R. Kim, H. Yoon, S. W. Kim, Y. J. Kim, Smart Wooden Home Enabled by Direct-Written Laser-Induced Graphene, Adv. Mater. Technol. 8 (2023) 2201952.

[S6] W. Zhao, Y. Jiang, W. Yu, Z. Yu, X. Liu, Wettability Controlled Surface for Energy Conversion, Small 18 (2022) 2202906.

[S7] L. Wang, K. Yin, Q. Deng, Q. Huang, C. J. Arnusch, Multiscale hybrid-structured femtosecond laser-induced graphene with outstanding photo-electro-thermal effects for all-day anti-icing/deicing, Carbon 219 (2024) 118824.

[S8] L. Wang, M. Liu, Y. Wu, H. Zheng, Asymmetrically superwetting Janus membrane constructed by laser-induced graphene (LIG) for on-demand oil-water separation and electrothermal anti-/de-icing, Chem. Eng. J. 488 (2024) 150862.

[S9] L. Huang, M. Gu, Z. Wang, T. W. Tang, Z. Zhu, Y. Yuan, D. Wang, C. Shen, B. Z. Tang, R. Ye, Highly Efficient and Rapid Inactivation of Coronavirus on Non-Metal Hydrophobic Laser-Induced Graphene in Mild Conditions, Adv. Funct. Mater. 31 (2021) 2101195.

[S10] Y. Chen, J. Long, B. Xie, Y. Kuang, X. Chen, M. Hou, J. Gao, H. Liu, Y. He, C. P. Wong, One-Step Ultraviolet Laser-Induced Fluorine-Doped Graphene Achieving Superhydrophobic Properties and Its Application in Deicing, ACS Appl. Mater. Interfaces 14 (2022) 4647–4655.